Astron. Astrophys. 303, 427–439 (1995)

ASTRONOMY AND ASTROPHYSICS

High-frequency radio continuum observations of radio galaxies with low and intermediate luminosities

III. Spectral indices and particle ages

U. Klein[1], **K.-H. Mack**[1], **L. Gregorini**[2,3], **and P. Parma**[2]

[1] Radioastronomisches Institut der Universität Bonn, Auf dem Hügel 71, D-53121 Bonn, Germany
[2] Istituto di Radioastronomia del C.N.R., Via P. Gobetti 101, I-40129 Bologna, Italy
[3] Dipartimento di Fisica, Via Irnerio 46, I-40126 Bologna, Italy

Received 27 December 1994 / Accepted 14 February 1995

Abstract. We have investigated the distributions of the spectral index across ten low- and intermediate-luminosity radio galaxies selected from the B2 catalogue. Some important source properties pertaining to the propagation and ageing of the relativistic particles have been derived. Most sources exhibit a spectral steepening towards the outer lobe regions, with spectral changes which are basically consistent with synchrotron ageing. However, the steepening is less pronounced as compared to that found for FRII sources. Typical source ages range from about 40 to 70 Myr. A few cases deviating from this behaviour are discussed.

A peculiar spectral index distribution is found in the giant radio galaxy 0136+39. The very steep spectrum throughout the source is reminiscent of a relict source, although it hosts a rather strong, but steep-spectrum, central source. The spectrum steepens strongly from the outer lobes towards the core, similar to what is seen in FRII radio galaxies.

The source 0828+32 possesses a young and an old lobe system. The peculiar morphology of 0828+32 is interpreted in terms of a precessing jet with decreasing length, consistent with the observed behaviour of the radio spectrum along its lobe system. This model is supported by the low upper limits of its core radio luminosity, and suggests that this source is in the process of exhaustion.

Key words: galaxies: active – quasars: general – radio continuum: galaxies

1. Introduction

Most investigations of the radio continuum spectra of radio galaxies were so far restricted to a frequency range below a few GHz. Essentially all of these studies were based on observations with interferometers which, however, become progressively insensitive to extended structure above this frequency regime. This has restricted spectral index studies to the low-frequency range ($\lesssim$1.4 GHz) and/or to sources of small ($\lesssim 5'$) angular extent.

Radio continuum spectra of radio galaxies contain important information about the source history. The observed variations in them are directly related to the mechanisms of particle energy losses and/or possible (re-)acceleration. The effects of energy buildup and losses of relativistic electrons have been extensively discussed in the seminal works of Kardashev (1962), Pacholczyk (1970; 1977) and Jaffe & Perola (1973). While the Kardashev and Pacholczyk (hereafter KP) model considers relativistic electrons which maintain their initial pitch angles against the magnetic field, the Jaffe & Perola (JP) model accounts for pitch angle isotropization throughout the lifetime of the radio source. Myers & Spangler (1985) have presented calculations of spectral steepening and corresponding particle ageing in the lobes of radio galaxies, based on two standard VLA observing frequencies. They did not argue in favour of any of the two models, but mostly presented results from the KP model, with additional comments on the JP one.

Maps of particle ages in radio sources, based on multi-frequency observations, have been published for a few bright FRII sources (see e.g. Jägers 1986; Alexander & Leahy 1986; Alexander 1987; Leahy et al. 1992; Carilli et al. 1991; Liu et al. 1992). These show the observations to be in accordance with the widely accepted view of particle acceleration in the hot spots of FRII sources, with subsequent energy losses of particles as they leak out into the lobe region and flow back towards the host galaxy. Katz-Stone et al. (1993) have recently questioned the classical techniques of utilizing the spectral steepening as a means to study particle ageing, and suggest a colour-colour analysis based on three-frequency measurements. Notwithstanding this discussion, we will proceed in the usual way of estimating particle ages by deriving spectral changes across our sources based on measurements at only two frequencies which are avail-

Send offprint requests to: U. Klein

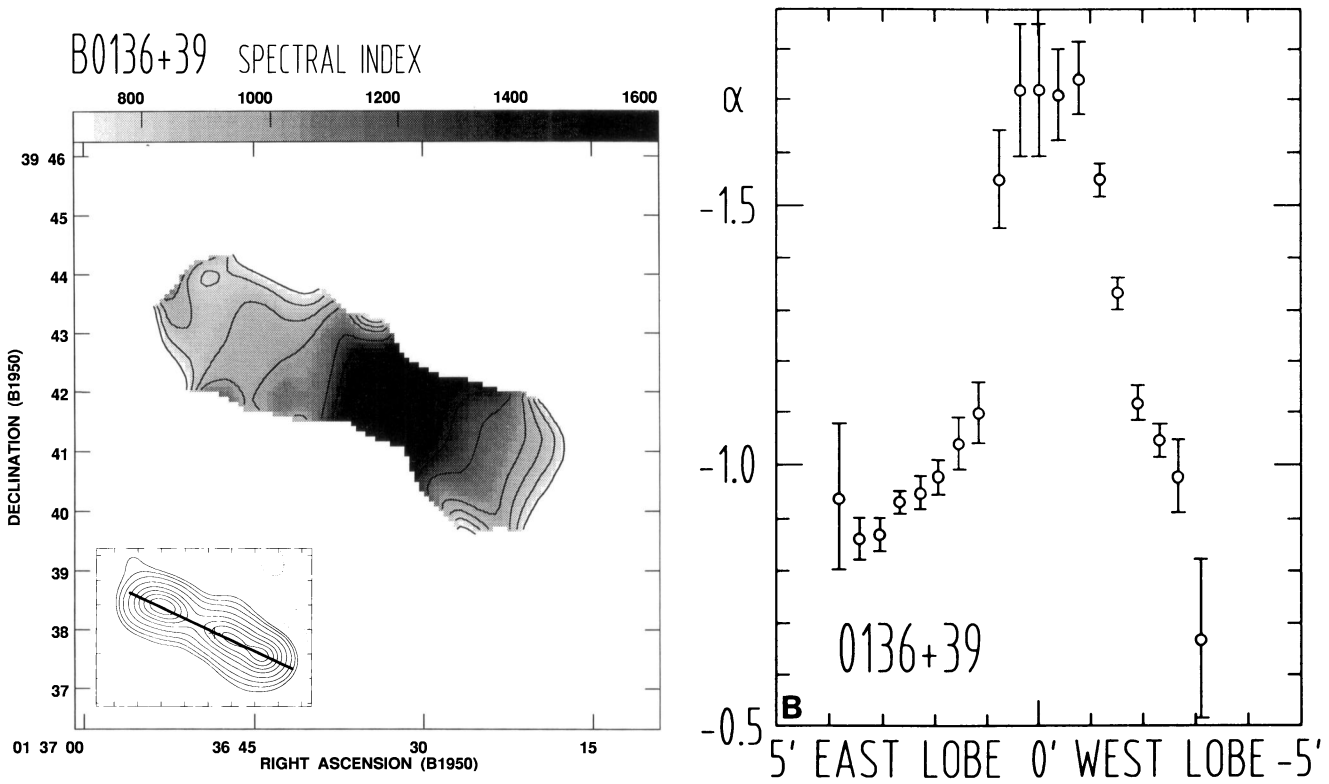

Fig. 1. a Map of the spectral index distribution across the radio galaxy 0136+39, derived between 20 cm and 2.8 cm wavelength. The cross indicates the nucleus of the source. The insert displays the contour map at $\lambda 20\ cm$. The hatched circle indicates the half-power beam size of the spectral index analysis. **b** Spectral index along the ridge line of the source as indicated in the insert of **a**

Table 1. Source parameters

Source	m [mag]	z	Distance [Mpc]	Diameter [kpc]
0136+39	19.5[a]	0.2107	522	1000
0204+29	16.5[a]	0.1090	295	320
0326+39	14.9[b]	0.0243	71	160
0828+32	14.8[a]	0.0507	145	270 × 500[c]
0836+29	14.7[a]	0.0790	220	430
1243+26	15.1[a]	0.0891	245	340
1321+31	12.7[b]	0.0161	48	160
1615+35	14.9[b]	0.0296	86	130
1827+32	15.1[a]	0.0659	185	320
2249+37	15.2[a]	0.0587	166	150

a:m_V
b:m_{pg}
c: extent of 'young' and 'old' lobes (see Sect. 2.5)

able. The advantage of our procedure is that we cover a wide frequency range, with a low and a very high radio frequency involved.

Studies of the spectral index distributions in low-luminosity (FRI) sources have been rare so far. A detailed multi-frequency analysis of 3C31 and 3C449 was published by Andernach et al. (1992). Bridle et al. (1991) have investigated the spectral index across the source B2 0326+39. These analyses have shown that the spectrum in low-luminosity sources steepens away from the source centres, contrary to the high-luminosity ones in which it steepens from the outer hot spots towards the host galaxy.

A comprehensive study of the ageing of particles in FRI sources has so far not been carried out. We have therefore begun to observe a sample of B2 sources at 2.8 cm wavelength, using the Effelsberg 100-m telescope (Gregorini et al. 1992; Mack et al. 1994, hereafter referred to as Papers I and II, respectively). Some of these sources had previously been observed at 49 cm with the WSRT and at 20 cm wavelength with the VLA, in its *D*-configuration. In this paper we investigate the distributions of the spectral index across ten such sources, based on these measurements. In Sect. 2 we describe the results for the individual sources. In Sect. 3 we discuss these and present a precession model for the peculiar cross-shaped source 0828+32. In Sect. 4 we summarize the main results and draw our conclusions. Throughout this paper we will assume a Hubble constant of $H_0 = 100\,\mathrm{km\,s^{-1}\,Mpc^{-1}}$ and a deceleration parameter of $q_0 = 1$.

2. Distributions of the spectral index

2.1. The measurements

The observational results which the present study is based on have been presented in previous papers. Observations of low-luminosity radio galaxies were carried out at $\lambda 49$ cm with the WSRT and reported by Fanti et al. (1981a,b; 1982), Parma et

al. (1985) and Bridle et al. (1991). A couple of 4C sources with intermediate luminosity have been observed at $\lambda 20$ cm with the VLA in its *D* configuration and have been presented by Bondi et al. (1993). The $\lambda 2.8$ cm measurements with the Effelsberg 100-m telescope were published by Gregorini et al. (1992) and by Mack et al. (1994). Prior to Fourier inversion and deconvolution the (*uv*)-ranges of the interferometric measurements have been cut off at 2.3 $k\lambda$, such as to match the illumination of the 100-m telescope at 2.8 cm wavelength. Maps with a Gaussian beam of size 69″ were produced in this way which can be directly compared to the Effelsberg maps. The latter have been CLEANed as indicated in Paper II (see also Mack et al., in prep.). Using the AIPS software package, the Effelsberg maps have then been interpolated onto the same grid as the WSRT and VLA data, and maps of the spectral index were subsequently produced. These will be described in the following subsection. Spectral index values have been computed for any map pixels for which both total power maps possessed at least a 3-σ intensity level. In addition, we have computed the spectral index and its error along the ridge lines of the sources by averaging the intensities at both wavelengths along these lines.

In Figs. 1 through 10 we present the spectral index maps, with the $\lambda 49$ or $\lambda 20$ cm maps as an insert, for each source, all furnished with the same angular resolution and sampling interval (3″ for the sake of quality of the display). Also shown are the spectral index values computed along the ridge line of each source (except for 2249+37, which has a rather complex structure at higher angular resolution (see Sect. 2.11)). These lines are indicated in the corresponding low-frequency maps shown in the inserts. The position of the central core is indicated by a cross in each map. All spectral indices α given here refer to the convention $S_\nu \sim \nu^\alpha$. The redshifts were published by Colla et al. (1975) and Fanti et al. (1977; 1978) for the B2 sources and by Gregorini et al. (1988) for the 4C sources. In Table 1 we have compiled some important source parameters. Column 1 contains the source name, Column 2 the apparent (visual or photographic) magnitude, Column 3 the distance, and Column 5 the source extent, estimated from the $\lambda 2.8$ cm maps.

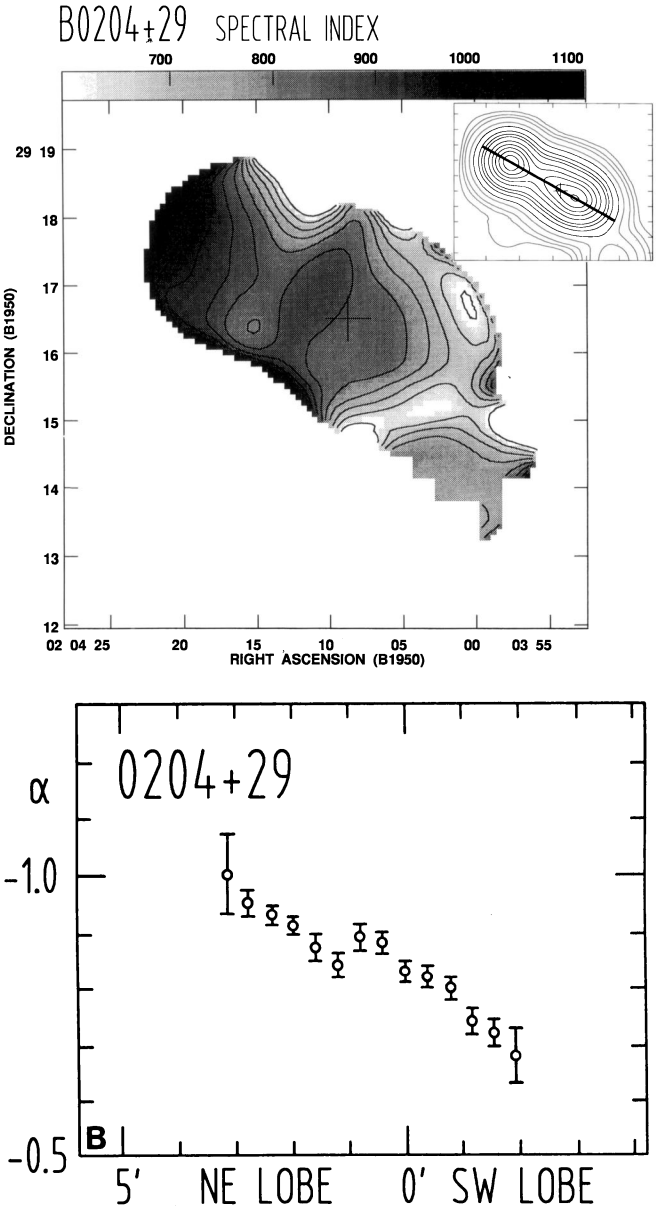

Fig. 2. a Map of the spectral index distribution across the radio galaxy 0204+29, derived between 20 cm and 2.8 cm wavelength. Layout is identical to that of Fig. 1a. **b** Spectral index along the ridge line of the source as indicated in the insert of **a**

2.2. 0136+39 (4C39.04)

In Fig. 1a the maps of 0136+39 (4C39.04) are displayed. The total angular extent of this source as judged from the $\lambda\lambda 20$ and 2.8 cm maps is about 8′, yielding a linear extent of ~1 Mpc, which ranks it among the largest known radio galaxies. As already noted in Paper II, the overall spectrum of 0136+39 is steep, and in particular the spectrum of the central source is unusually steep. This is evident in Figs. 1a and b, in which the distribution of the spectral index between $\lambda 20$ cm (data from Bondi et al. 1993) and $\lambda 2.8$ cm is displayed. The NE lobe has a mean spectral index $< \alpha >= -0.94 \pm 0.06$, the NW one $< \alpha >= -1.05 \pm 0.07$. Some evidence is found for a flatter spectrum ($\alpha \sim -0.6$ to -0.7) towards the outer peripheries of the lobes. An essentially constant spectrum is seen perpendicular to the source major axis.

The central region is characterized by an usually steep spectrum. This is most probably caused by the contamination at $\lambda 20$ cm of the lobe which has a steeper spectrum than the core. The flux densities of the core measured at $\lambda\lambda 20$ and 6 cm (Bondi et al. 1993) yield a spectral index of -0.88. Our comparison between the $\lambda\lambda 20$ and 2.8 cm data implies a further rapid steepening towards shorter wavelengths, with $\alpha = -1.72 \pm 0.10$. This is quite unusual for core regions of extended radio sources, indicating that the structure is rather complex (Saripalli et al., in prep.).

2.3. 0204+29 (4C29.06)

The spectral index distribution of this source, derived between $\lambda 20$ cm (data taken from Bondi et al. 1993) and $\lambda 2.8$ cm, is shown in Fig. 2. A gradual steepening of the spectrum from $< \alpha >= -0.70 \pm 0.03$ in the SW lobe to $< \alpha >= -1.00 \pm 0.04$ in the NE one is evident. In the SW, at least part of this flattening may be related to the presence of a presumably unrelated background source (see Meurs & Wilson 1981; Meurs & Unger 1991; Gregorini et al. 1988). The measured spectral index values indicate a steepening of the total source spectrum between $\lambda\lambda 20$ and 2.8 cm if compared with the overall total source spectrum, which has $< \alpha >= -0.58 \pm 0.05$ (see Paper II). The spectral index does not vary strongly perpendicular to the major axis. The core region, which is probably related to a Seyfert galaxy (Meurs & Wilson 1981), does not particularly show up in the spectral index distribution. The background source located at $\alpha_{50} = 02^h04^m01^s.1$, $\delta_{50} = 29°14'10''$ has $\alpha = -0.8 \pm 0.1$.

2.4. 0326+39

A spectral index study of this source in the range between 49 and 6 cm wavelength was contained in the work of Bridle et al. (1991). Our spectral index data (with the $\lambda 49$ cm map of Bridle et al. involved) confirm the general trend between $\lambda\lambda 49$ and 21 cm derived by those authors. The central region which blends the core and the central bright jet into the beam size of the present work shows the flattest spectrum, with $\alpha = -0.46 \pm 0.02$. A slight asymmetry between the two lobes is seen in Fig. 3. The eastern lobe has a mean spectral index $< \alpha >= -0.85 \pm 0.04$, in the western one we find $< \alpha >= -0.73 \pm 0.05$.

Our spectral index map (Fig. 3a) furthermore shows evidence for a lateral steepening of the source spectrum, away from the major axis. This is probably caused by the steep spectrum component that extends around the source (see the insert in Fig. 3a or Fig. 1 of Bridle et al. 1991). These particles are likely to have diffused away from the lobes. The high-resolution maps published by Ekers et al. (1981, their Fig. 5) and by Bridle et al. (1991, their Fig. 5) exhibit an overall 'S'-symmetry of the lobes, with the magnetic field following the outer bends of the lobes (see Fig. 3a of Paper I – rotating the E-vectors displayed there by 90°).

2.5. 0828+32

Our $\lambda 2.8$ cm data, which were first obtained by Gregorini et al. (1992) and superseeded by a more sensitive map by Mack et al. (1994) in order to trace the presumably old lobes of this peculiar radio galaxy, has been compared with the 49 cm data of Parma et al. (1985). The results of the first thorough spectral index study of this source are presented in Fig. 4. At this resolution the peculiar old lobe is very prominent (see the insert in Fig. 4a). The $\lambda 2.8$ cm map (see Fig. 3 in Mack et al. 1994) was in fact sensitive enough to detect this feature both, north and south of the source's major components. The projected magnetic field orientation, free from Faraday effects at

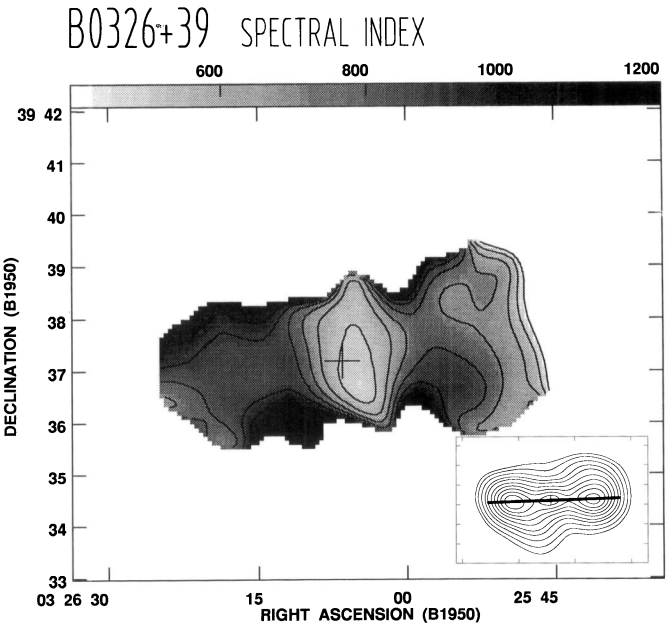

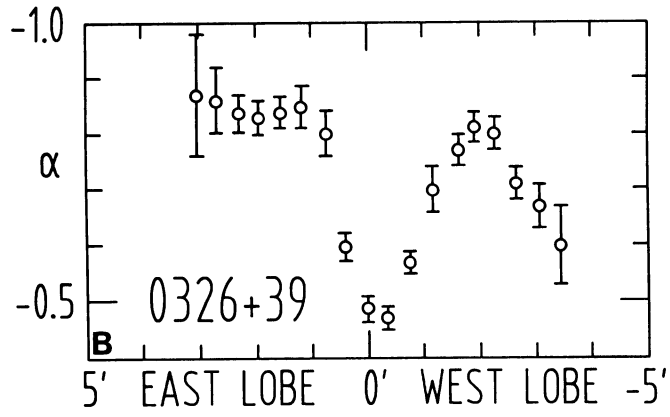

Fig. 3. a Map of the spectral index distribution across the radio galaxy 0326+39, derived between 49 cm and 2.8 cm wavelength. Layout is identical to that of Fig. 1a. **b** Spectral index along the ridge line of the source as indicated in the insert of **a**

2.8 cm wavelength, was found to lie along the giant old lobes, and perpendicular to the presumed young lobes. The spectral index distribution (Fig. 4) clearly shows a rapid steepening of the spectrum along the old lobes, from $< \alpha >= -0.68 \pm 0.02$ in the young lobes to extreme values of $\alpha = -1.05 \pm 0.15$ in the northern old lobe and $\alpha = -1.16 \pm 0.15$ in the southern. Thus, the spectra in the old lobes are not quite as steep as measured by Parma et al. (1985); it is possible that their 21 cm observations with the WSRT suffered from short spacing problems, which may be severe for these very extended components. Clear evidence is found for spectral gradients in both of these lobes, with a steeper gradient in the northern one, except for the feature located at $\alpha_{50} = 08^h28^m12^s$, $\delta_{50} = 32°34'11''$, which becomes visible again at $\lambda 2.8$ cm. Along the source's major axis, i.e. along the young lobes, the average spectrum varies only very little between $< \alpha >= -0.68 \pm 0.02$ in the lobes

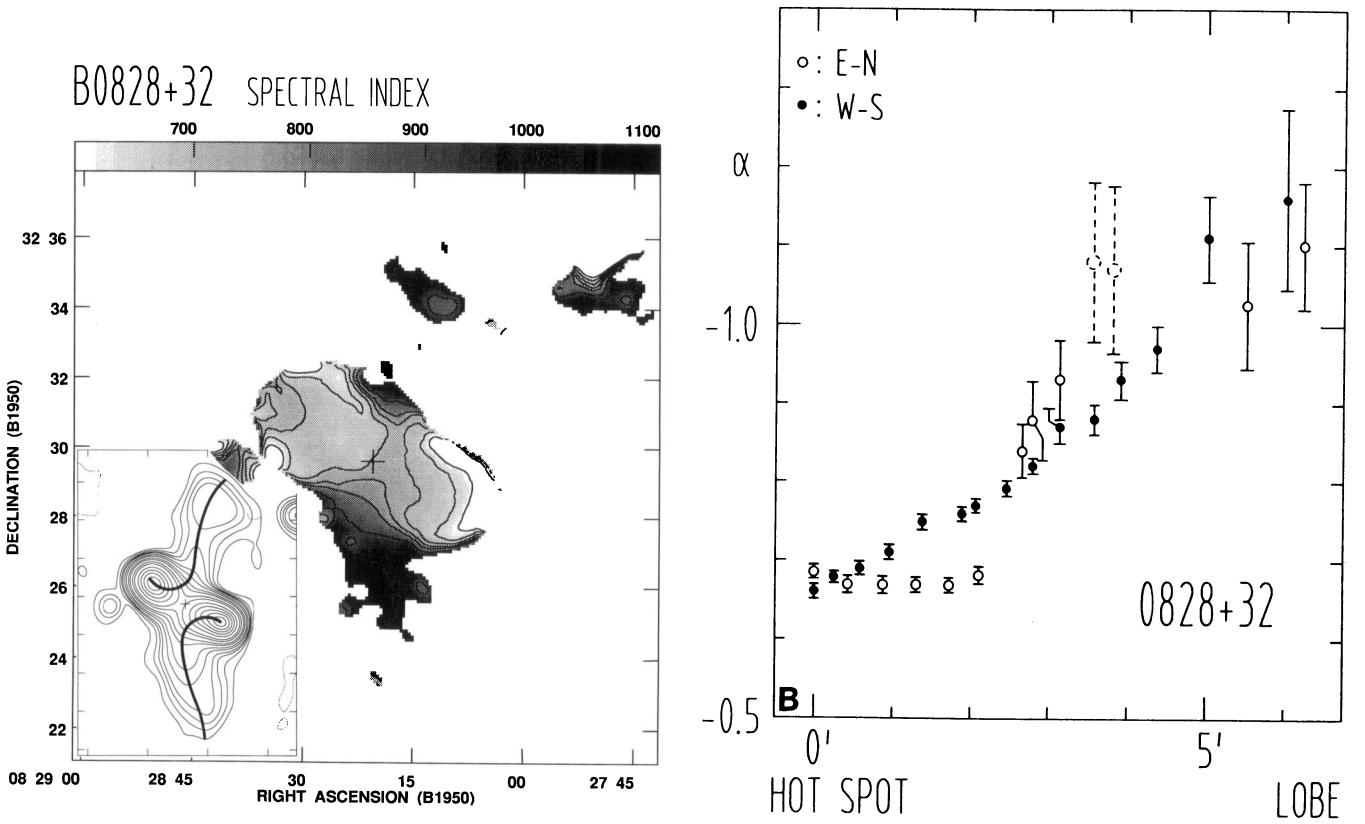

Fig. 4. a Map of the spectral index distribution across the radio galaxy 0828+32, derived between 49 cm and 2.8 cm wavelength. Layout is identical to that of Fig. 1a. **b** Spectral index along the paths connecting the 'young' and 'old' lobes as indicated in the insert of **a**. Filled circles trace the spectrum from the eastern young into the northern old lobe, open circles show that from the western young into the southern old lobe. The two dashed symbols in the northern lobe have a higher uncertainty, owing to the low signal-to-noise ratio there

and $< \alpha >= -0.75 \pm 0.03$ in the central region. This agrees well with the findings of Parma et al. (1985). In Sect. 3.1 we discuss the likely physical origin of the source morphology of 0828+32. To this end, we have determined the spectral index values along the ridge lines connecting the hot spot region in each young lobe to the corresponding old one (see Sect. 3.1 for details). These spectral indices are displayed in Fig. 4b.

2.6. 0836+29

The spectral index data of this source, obtained by comparing with an unpublished WSRT map at 49 cm, are shown in Fig. 5. Valentijn (1979) classified it as a wide-angle tail (WAT) source. The core shows a flat spectrum, with $\alpha = -0.16 \pm 0.02$. The spectrum gradually steepens along the source ridge to the outer lobes, with extreme values of $\alpha = -0.95 \pm 0.04$ in the NE lobe end, and $\alpha = -1.05 \pm 0.08$ in the SW one. This steepening is faster towards the north than towards the south. The flattening present at about 2′ from the core in the south-west lobe corresponds to a peak in the brightness at the location of the sharp southern bend, where the magnetic field is probably compressed as suggested by the high degree of linear polarization seen there (Paper II). Taking together the marked S-shape of the source (see in particular the map of de Ruiter et al. 1986) and the spectral steepening towards the outer lobes, this may be interpreted in terms of precession of the jets, with the precession axis nearly in the plane of the sky.

2.7. 1243+26

The spectral index data of this asymmetric source, computed using an unpublished WSRT λ49 cm map, are displayed in Fig. 6. We probably witness here the superposition of two sources convolved to a single one at our resolution of 69″ to give the impression of a single complex source. The positions of the cores of the host galaxies are indicated in Fig. 6 (see Fig. 2 of Fanti et al. 1987 for a detailed high-resolution map showing the two cores). The two individual sources still have a complex morphology at higher resolution, which is explicable in view of their membership of the galaxy cluster A1609. We have computed the spectral indices roughly along the ridge line of the two outer tails as well as along the southern extension and show them in Fig. 6b. The source located north of 1243+26 is an unrelated background object.

The spectral index is flattest around the two core positions, with $\alpha = -0.55 \pm 0.03$ in the northern and $\alpha = -0.60 \pm 0.03$ in the southern head of the two sources. Away from the brightest regions seen in the insert of Fig. 6a the spectrum steepens rapidly to $< \alpha >= -1.0 \pm 0.15$, thus reflecting the ageing of the particles along the tails.

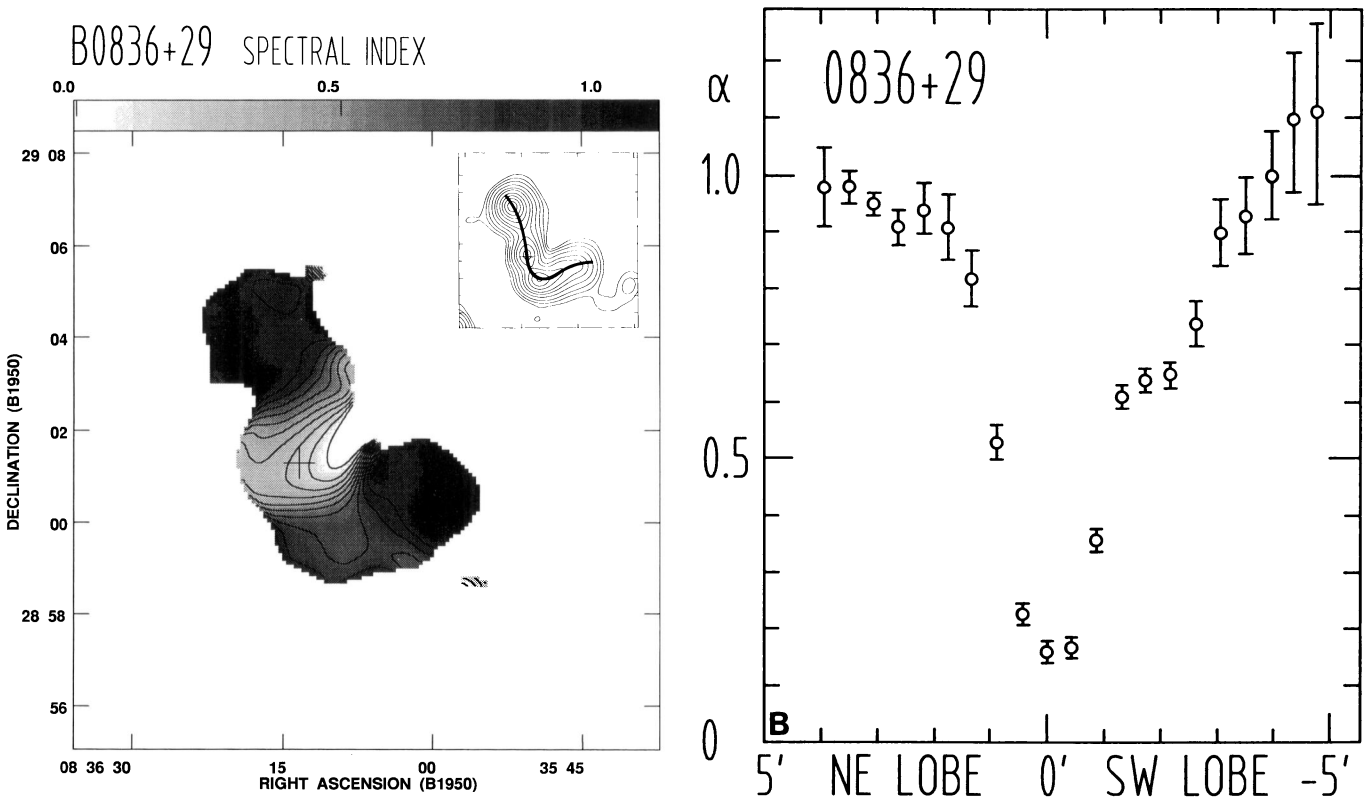

Fig. 5. a Map of the spectral index distribution across the radio galaxy 0836+29, derived between 49 cm and 2.8 cm wavelength. Layout is identical to that of Fig. 1a. **b** Spectral index along the ridge line of the source as indicated in the insert of Fig. 2a

2.8. 1321+31

The λ49 cm map obtained with the WSRT by Fanti et al. (1982) was used to derive the spectral index distribution of this source. Here we are faced with another case of a source showing a spectral steepening perpendicular to the major axis. Figure 7a shows little variation of the spectrum along the major axis. The central region which at our resolution encompasses the nucleus and the inner jet has a fairly flat spectrum, with $< \alpha >= -0.56 \pm 0.02$. A steepening to $< \alpha >= -0.64 \pm 0.03$ is found at about 1′.3 away to either side on the ridge of the source, with a marginal flattening occurring at the outermost periphery (see also Fig. 7b). Comparison with the values derived by Fanti et al. (1982) between 49 and 21 cm suggests a steepening of the spectrum along the major axis towards higher frequencies, and does not confirm the flatter spectrum which they obtained between $\lambda\lambda$21 and 6 cm which is likely to reflect the spectrum of the small-scale structure, viz. the jet. The lack of the extended component at λ2.8 cm (see Fig. 8a in Paper I) results in an overall steepening of the spectrum away from the major axis, as is readily seen in Fig. 7a. On average, values of $< \alpha >= -0.75 \pm 0.11$ are measured at about 1′.6 distance from the major axis, with extreme values of ~ -1.0 in the NW part of the source.

2.9. 1615+35

The 49 cm map of this source (see insert in Fig. 8a), published by Ekers et al. (1978), was used to produce the spectral index distribution. The spectral index map is shown in Fig. 8a. A gradual steepening of the spectrum is observed from the position of the host galaxy to the outer end of the tail, as far as it can be traced in our λ2.8 cm map.

Ekers et al. (1978) have conducted a thorough spectral index study of this tailed radio source using data obtained with the WSRT at 3 wavelengths ($\lambda\lambda$49, 21, and 6 cm). They argued that in case of 1615+35 there may be particle re-acceleration within the tail, based on the incompatibility of the derived particle ages (from the spectral index distribution) and the likely galaxy and Alfvén velocities. Our results confirm the spectral indices derived by those authors between 49 and 21 cm wavelength (see Fig. 8b). Figure 8a shows that out to about 5′.5 the high-frequency spectrum steepens more rapidly than the low-frequency one (cf. Fig. 4a of Ekers et al. 1978), beyond this distance the tendency for a roughly constant spectrum at about $\alpha = -1.2 \pm 0.1$ is indicated.

2.10. 1827+32

A λ49 cm WSRT map of Parma et al. (unpublished data) was used to derive the spectral index distribution of this source. This map is displayed in the insert of Fig. 9. As already indicated in

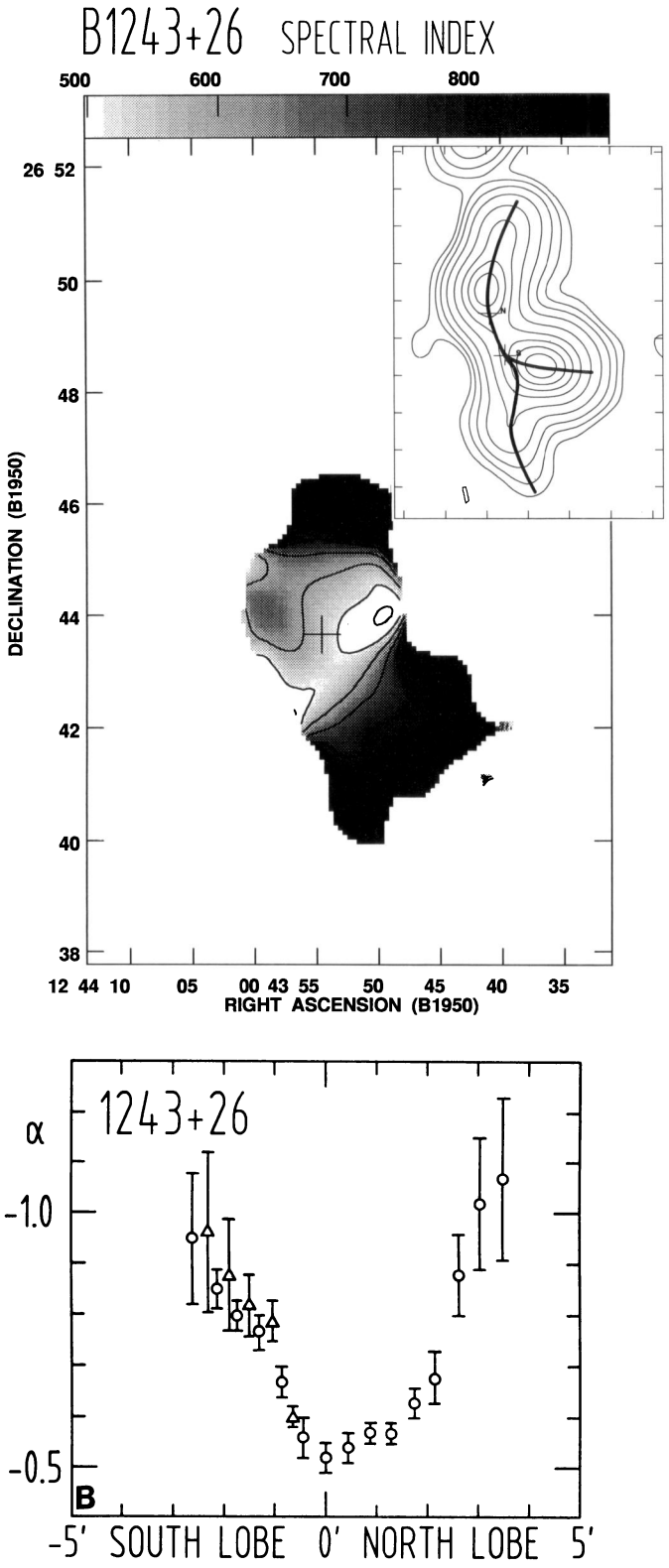

Fig. 6. a Map of the spectral index distribution across the radio galaxy 1243+26, derived between 49 cm and 2.8 cm wavelength. Layout is identical to that of Fig. 1a. **b** Spectral index along the ridge line of the source as indicated in the insert of **a**. Triangles correspond to the southern extension

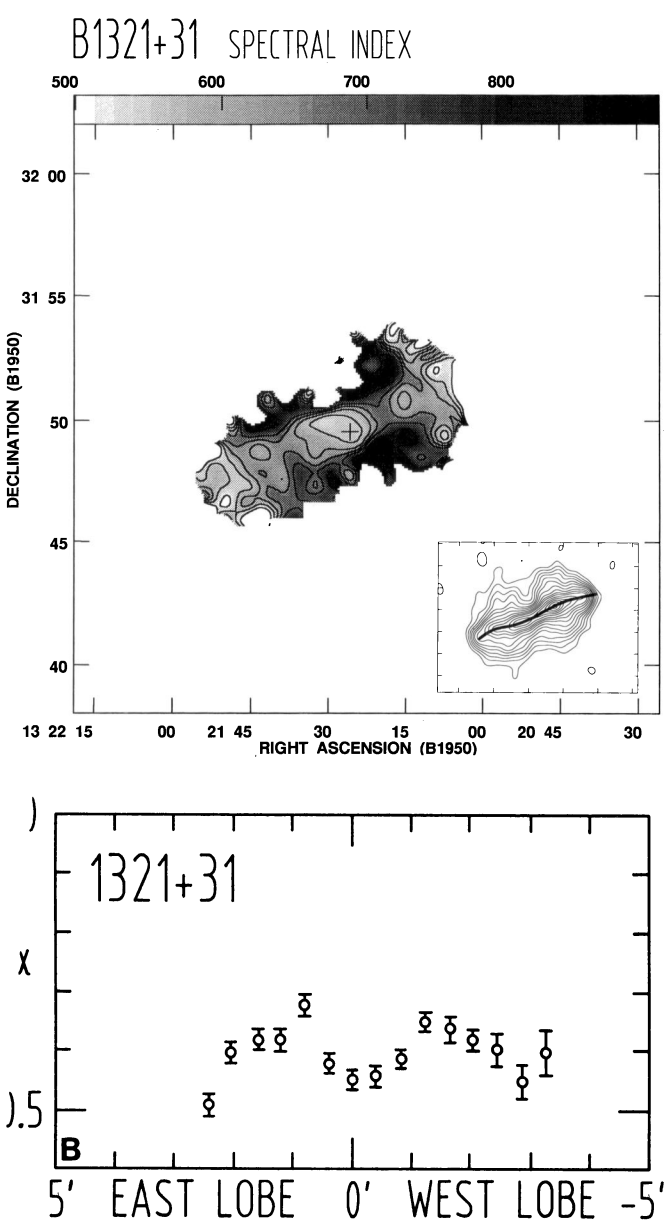

Fig. 7. a Map of the spectral index distribution across the radio galaxy 1321+31, derived between 49 cm and 2.8 cm wavelength. Layout is identical to that of Fig. 1a. **b** Spectral index along the ridge line of the source as indicated in the insert of **a**

Paper I, the spectrum in the central region is rather flat, with a spectral index of $\alpha = -0.35 \pm 0.04$. Away from this region the spectrum steepens rapidly to $< \alpha >= -0.76 \pm 0.05$ in the southern and northern lobes (Figs. 9a and b).

2.11. 2249+37 (4C37.66)

Katgert-Merkelijn et al. (1980) first noted the unusually complex structure of this source. A more detailed map was recently obtained by Bondi et al. (1993) with the VLA at 20 cm wavelength. The morphology visible presents a point source precisely coinciding with the position of the optical identification of Katgert-Merkelijn et al. (1980), and a low-brightness struc-

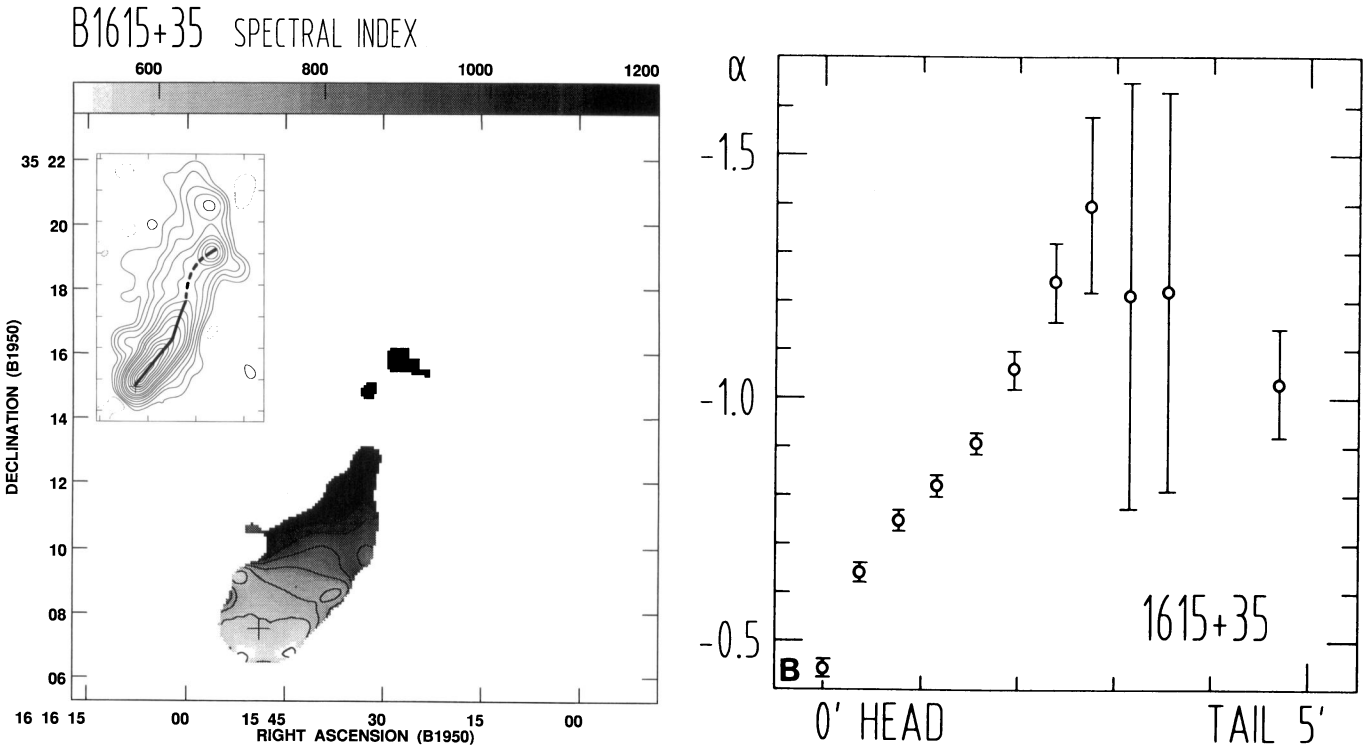

Fig. 8. a Map of the spectral index distribution across the radio galaxy 1615+35, derived between 49 cm and 2.8 cm wavelength. Layout is identical to that of Fig. 1a. **b** Spectral index along the ridge line of the source as indicated in the insert of **a**

ture extending to the south. Our spectral index map (Fig. 10) appears to support the hypothesis of 2249+37 being a head-tail source. The spectrum is flattest in the NE, close to the presumed nucleus, with $\alpha = -0.43 \pm 0.09$. It steepens systematically towards the SW, with the lowest values occurring close to the locations of the broad tails. Thus, values of $< \alpha >= -0.73 \pm 0.04$ and $< \alpha >= -0.76 \pm 0.02$ are found in the regions around $\alpha_{50} = 22^h49^m08^s$, $\delta_{50} = 37°56'.6$ and $\alpha_{50} = 22^h49^m01^s$, $\delta_{50} = 37°56'.4$, respectively.

3. Discussion

3.1. Particle ageing

In this section we shall try to interprete the results of our spectral analysis of B2 and 4C radio galaxies in terms of particle ages and source lifetimes. To this end, we will estimate the break frequency ν_b along the main ridge of each source. The observed spectral index α will be compared with the presumed injection index α_{inj} at equi-distant locations along these ridges, with $\alpha_{inj} = -0.6$. The two 'standard' models of particle ageing, the so-called KP and JP models (see e.g. Carilli et al. 1991, and Sect. 1) are usually applied to calculate break frequencies. We shall calculate ν_b for the KP model. With only two frequencies involved we cannot yet distinguish between the two models. The required magnetic field strengths have been computed via the usual assumption of equipartition between particles and fields, utilizing the formula of Miley (1980):

$$B_{eq} = 7.91 \cdot \left[(1+k) \cdot (1+z)^{3-\alpha_{inj}} \cdot \frac{S_o}{\nu_o^{\alpha_{inj}} \cdot \theta_x \cdot \theta_y \cdot s} \cdot \frac{\nu_u^{\alpha_{inj}+1/2} - \nu_l^{\alpha_{inj}+1/2}}{\alpha_{inj} + 1/2} \right]^{2/7} \quad \mu G$$

Here, z is the redshift, S_o is the flux density (in mJy) at some frequency ν_o (in GHz), k is the ratio of the energy content of relativistic protons to that of electrons (adopted as k=1), ν_l and ν_u are the integration boundaries for the radio luminosity (ν_l = 10 MHz ν_u = 100 GHz used here), s is the line-of-sight (in kpc), and θ_x and θ_y is the source extent in two directions, measured in arcsec. The break frequencies were computed by using analytical approximations to the functions tabulated by Pacholczyk (1977), and assuming an injection index $\alpha_{inj} = -0.6$. From the break frequencies the ages τ follow as (Van der Laan & Perola 1969):

$$\tau = 1.59 \cdot 10^3 \cdot [\nu_b \cdot (1+z)]^{-0.5} \cdot \frac{B_{eq}^{0.5}}{B_{eq}^2 + [B_m \cdot (1+z)^2]^2} \quad \text{Myr}$$

Here, B_{eq} is the equipartition field (in μG), B_m the equivalent field of the 2.7-K background radiation (in μG), and ν_b the break frequency (in GHz). Table 2 summarizes the values of α, ν_b, and τ for each source. The values for the JP model are roughly speaking a factor of 3 higher for the break frequencies and a factor of 2 lower for the particle ages.

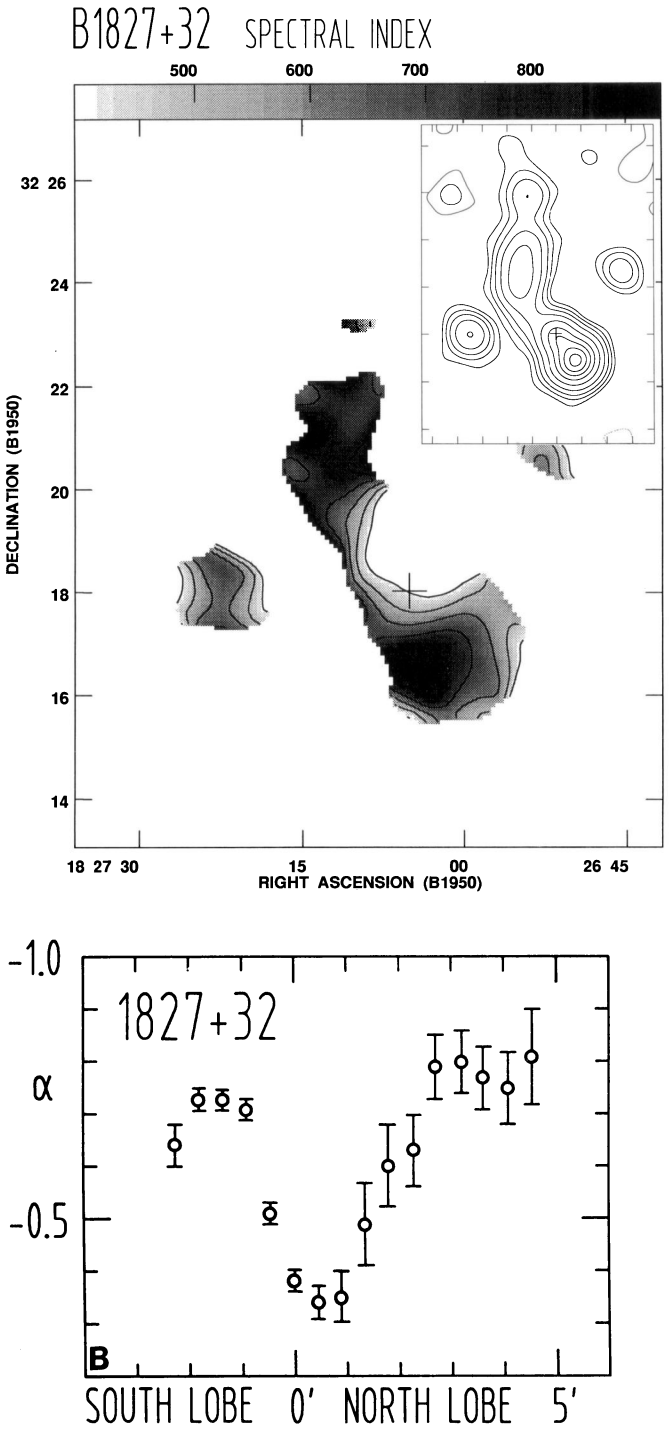

Fig. 9. a Map of the spectral index distribution across the radio galaxy 1827+32, derived between 49 cm and 2.8 cm wavelength. Layout is identical to that of Fig. 1a. **b** Spectral index along the ridge line of the source as indicated in the insert of **a**

Table 2 shows that the KP model yields particle ages of between about 40 and 70 Myr. for most of the sources. The only exception is 1615+35, the spectrum of which suggests an age of about 100 Myr. at the outer periphery of the tail. This is also visible in Fig. 11, where we have plotted the spectral indices for all of the sources (except for 0136+39, which has a peculiar spectral index distribution, and 0204+29, which is most likely confused with a background source) versus distance from their central cores. Jägers (1986) presented a similar plot for a sample of FRII sources, where he showed the spectrum as a function of distance from the hotspots *towards their cores*. Figure 11 exhibits a clear difference between low- and high-luminosity radio galaxies: while Jägers (1986) found a strong steepening of the spectrum *from the outer hotspots towards the inner cores* on scales of $\sim$ 200 to 300 kpc, the B2 and 4C sources exhibit a steepening *from the cores to the outer lobes*. The steepening is also much less pronounced in our sample, with the exception of 1615+356, even though our analysis includes a much higher radio frequency! In Fig. 11 a gradual steepening to $\alpha \sim -1.0$ is seen, while the low-frequency study of Jägers (1986) yields spectra as steep as $\alpha \sim -1.5$ between $\lambda\lambda$49 and 21 cm. A similar trend is only seen in 1615+35, which is a head-tail source (see Paper I).

The overall distribution of the spectral index across 0136+39 is reminiscent of FRII sources, in which the spectrum usually steepens from the lobe region towards the core. However, the overall spectrum between $\lambda\lambda$ 20 and 2.8 cm is very steep (see Sect. 3.1.1), showing no evidence at all for any contribution by a hotspot, where the spectrum would be expected to be significantly flatter. Therefore, the particle age of this source given in Table 2 should not be taken too seriously, as it is based on the assumption of an injection spectrum with -0.6 (s.a.). Such a spectrum is seen nowhere in the source, which would in the first place suggest that the central activity had been switched off some time ago. However, the λ20 cm map of Gregorini et al. (1988) shows a fairly strong (but steep-spectrum) central source, with a monochromatic radio luminosity of $\sim 10^{24}$ W Hz^{-1} at 1.4 GHz.

The source 0204+29 has a most peculiar spectral index behaviour. The north-eastern lobe (component 'A' in Meurs & Wilson 1991) shows a relatively steep spectrum (see Fig. 2). The spectrum gradually flattens towards the south-west. Given that the south-western component is the extended lobe of the one-sided jet seen at higher resolution, which is strongly suggested by the maps of Gregorini et al. (1988) and Bondi et al. (1993), then the opposite trend would be expected. We conclude that the particle ages calculated for this source are probably not very reliable because of the confusion problem.

The observed spectral indices of the 0326+39 between $\lambda\lambda$49 and 2.8 cm are in the range $\alpha = -0.80$ to -0.85. The particle ages resulting are 40 to 50 Myr. (Table 2). In order for the relativistic particles to reach their current locations which are some 60 to 70 kpc away from the lobe centres, they would have to have propagated with average speeds of ~ 2500 km s^{-1}.

The source 0828+32 deserves a more detailed discussion, which we conduct in Sect. 3.2.

In 0836+29 the estimated particle age (Table 2) leads to a propagation speed of at least (accounting possibly complex projection of the source) $\sim$1000 km s^{-1}. This could be even higher if the particles were re-accelerated at the locations of the bends in the source discussed in Sect. 3.3.

Table 2. Source parameters

Source	Region	α	B_c [μG]	ν_b [GHz]	τ [Myr]
0136+39	OL	−0.83	1.6	7.4	27
"	C	−1.72	2.0	1.7	62
0204+29	OL	−0.82	2.2	7.3	41
0326+39	OL	−0.75	2.7	7.2	45
0828+32	NL	−1.14	1.4	3.1	74
"	SL	−1.04	1.6	3.8	69
0836+29	OL	−1.02	2.0	4.0	62
1243+26	OL	−0.95	1.7	4.6	55
1321+31	OL	−0.63	3.0	10.9	47
1615+35	OT	−1.28	1.9	2.2	90
1827+32	OL	−0.74	1.7	7.7	47

OL: outer lobes; C: centre; NL: north lobe;
SL: south lobe; OT: outer tail

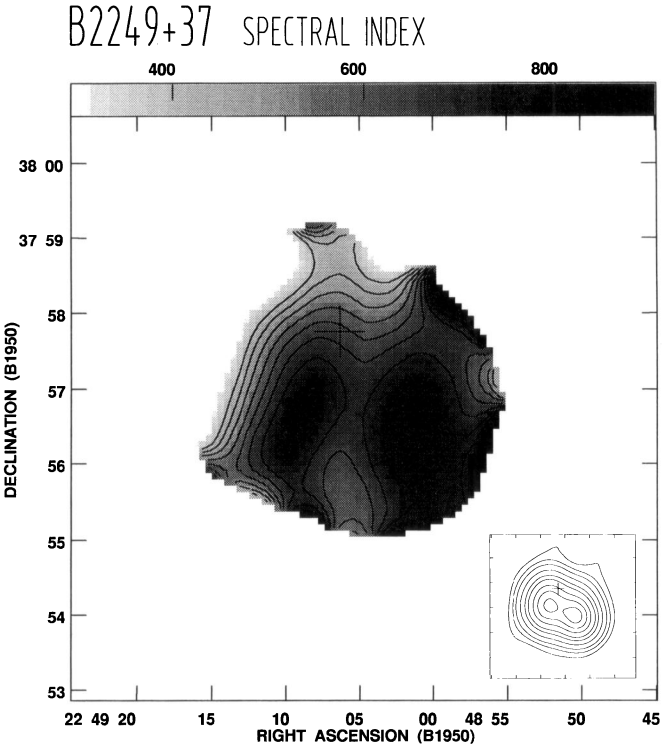

Fig. 10. Map of the spectral index distribution across the radio galaxy 2249+37, derived between 20 cm and 2.8 cm wavelength. Layout is identical to that of Fig. 1a

Similar to the situation in 0836+29, we note that the spectrum of 1243+26 remains flat at the location of the sharp bend (see Fanti et al. 1986, 1987; de Ruiter et al. 1986) of the northern jet, before it rapidly steepens into the outer lobe. It is again at this position that we observe strong linear polarization (Paper II), indicating compression of the magnetic field. By the same token, the particles will probably experience re-acceleration within this region. In contrast, the apparent bend in the southern source, immediately south of the southern core, is most likely a projection effect. Neither does our polarization map (Paper II) exhibit particularly strong linear polarization at this location, nor does the

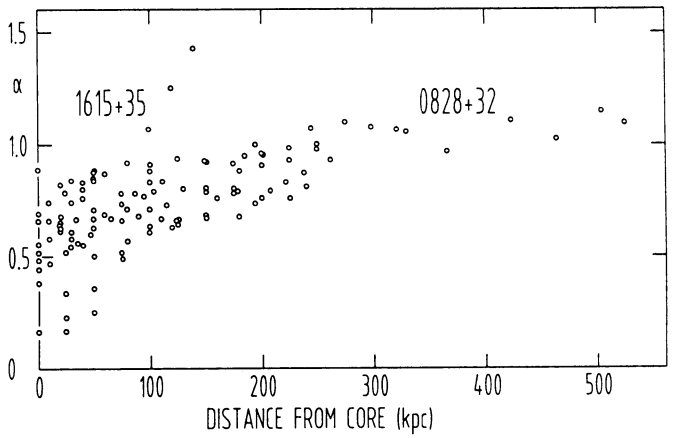

Fig. 11. Spectral indices of the sample sources, plotted versus linear distance from their cores. 0136+39 is not included (see text)

spectral index map show a flatter spectrum there as is seen at the location of the southern bend in 0836+29. The estimated particle speeds, using the age in Table 2, is $\sim$1000 km s^{-1}.

Fanti et al. (1982) have argued that the bulk of the kinetic energy transported by the jets of 1321+31 is deposited in its broad components, with the material flowing across the jet boundaries. This picture is strongly supported by our data. Along the jet the particles have a constant energy spectrum. Once they leave the jet regime, there is no longer replenishment of energy so that their energy content is quickly radiated away. The lateral flow is probably alleviated by the ubiquitous perpendicular orientation of the magnetic field all along the source. While Table 2 gives the particle ages at the outer ridges of the lobes, the spectra away from the ridge line are significantly steeper. Our observed average spectral index of the aged particles of −0.8 as compared to the injection spectrum of $\sim$ −0.64 on the source major axis suggests a particle age of about $6 \cdot 10^7$ yr, where a break frequency around 6 GHz and an equipartition magnetic field strength of 1.8 μG has been estimated for the outer extended components. This time scale is in the same range as the propagation time inferred from the projected distance of the particles from the jets and the Alfvénic velocity estimated by Fanti et al. (1982).

Our polarization measurements of 1615+35 at λ2.8 cm have uncovered high degrees of linear polarization along the tail of 1615+35, up to 50% within the outermost detectable region (see Paper I). The magnetic field orientation seen within the highly polarized region is clearly oriented along the tail so that the particles may easily diffuse along the highly ordered field. The observed degrees of polarization which are certainly free from Faraday effects do not leave much room for random components so that the quest for re-acceleration by hydro-magnetic turbulence (Fanti et al. 1981) remains a problem. The particle speed resulting from the age in Table 2 is only $\sim$110 km s^{-1}.

In the southern and northern lobes of 1827+32 the fine structure of the source becomes complex (see Fig. 47 of de Ruiter et al. 1986). It is in these regions that the jets become strongly deflected to produce the overall S-type morphology. Apparently the particles are subject to strong synchrotron losses in the bend-

ing magnetic field. In fact, the observed degrees of linear polarization are rather low in the source (see Parma et al. 1985 and Paper I), corroborating the supposition that the magnetic field is rather tangled over most of the source. The particle propagation speeds estimated from the age in Table 2 is $\sim$2500 km s^{-1}.

3.2. A precessing jet in 0828+32

By comparing the polarization map at 2.8 cm wavelength (Fig. 3b of Mack et al. 1994) with the distribution of the spectral index (Fig. 4a) it is evident that the projected magnetic field follows the steepest spectral index quite closely, thus probably delineating the path along which the ageing particles diffuse out into the old lobes. Figure 4a shows that the steepening of the spectrum is faster in the northern than in the southern old lobe. This may be related to the fact that the magnetic field is less ordered here than in the southern one (Mack et al. 1994): particles propagating along the northern lobe experience a somewhat more turbulent magnetic field and may thus lose energy more quickly.

Parma et al. (1985) have briefly discussed the possible origin of the secondary lobe system in 0828+32. At first glance, the existence of two apparently distinct lobe systems in this source may suggest a 'sudden' change in the ejection direction of the jets. This situation is, however, difficult to explain, in particular in view of the lack of any companion galaxy in the vicinity of the host galaxy of the radio source (Parma et al. 1985; Leahy & Parma 1992).

An alternative explanation is the precession of the central object, which would cause the hot spot of each jet to 'paint' the trace of the shocked region as two projected circles on the sky. In order for this hypothesis to be applicable to the situation in 0828+32, a special geometry concerning the orientation and opening angle of the precession cone has to be invoked. In the following we will show that the existing data on 0828+32 do in fact support the precession hypothesis. Parma et al. (1985) argued that the main difficulty with the precession model is the sharp transition from the young to the old lobes and the lack of any gradual spectral steepening in this source, which is much more evident e.g. in NGC 326 (Ekers et al. 1978). However, the λ20 cm map of Machalski & Condon (1985) provides clear evidence for a continuous transition between the young and the old lobes. Furthermore, the observed spectral index between $\lambda\lambda$49 and 2.8 cm along the lobe systems as derived in Sect. 2.5 strongly suggests a gradual steepening from an injection spectrum with $< \alpha >= -0.68$ in the hot spot regions (young lobes) to $< \alpha >= -1.12$ at the old lobes' terminations. We may also consider the magnetic field as observed at λ2.8 cm (Paper II) in the old lobes as a relic of the compressed field in the hot spots. According to Table 2 our estimate of the particle age in the old lobes is $\sim$70 Myr.

Inspection of Fig. 2 of Parma et al. (1985; see also the insert in our Fig. 4a) readily shows that the (projected) sections of the trajectories swept out by the ends of the pair of beams deviate significantly from the expected shape. These would form ellipses, with their major axes perpendicular to the axis of the precession cone (see the sketch shown by Ekers et al. 1985; their Fig. 2). First, there seems to be an overall distortion of the outer lobe regions towards the west, which may be the result of the galaxy's relative motion through an intergalactic medium. Such lateral deviations are frequently encountered in extended radio sources. Second, the observed morphology strongly deviates from an ellipse, and the major axis of the presumable ellipse is *not* perpendicular to the precession axis. We therefore suggest that the best way to explain this structure is to assume that the length of the precessing beams changes with time: the (projected) distance of the hot spots from the galaxy has *decreased* from the outermost old lobes to the present location of the hot spots! In this context, it is important to note that the core of 0828+32 is one of the weakest in low and intermediate luminosity radio sources (see Feretti et al. 1984), with upper limits to the flux density of the core of 3 mJy at λ6 cm (Feretti et al. 1984) and 2 mJy at λ13 cm (Wehrle et al. 1984). The monochromatic luminosity of the core is $< 8.3 \cdot 10^{21}$ W Hz^{-1} at 6 cm wavelength, only 3.6 times above the upper limit to the core luminosity of the prototypical relic radio galaxy 0924+30 (see e.g. Cordey 1987). It is tempting to associate the likely exhaustion of the central engine with the apparent shortening of the beams in 0828+32. With these premises in mind one can easily understand the overall structural and spectral properties of the source.

In Fig. 12 we sketch the likely situation that we are witnessing in 0828+32. Here the precession axis is pointing towards us in the north-east. The situation could obviously be reverse, which cannot be decided. The sketch depicts the structure in the absence of ram pressure effects, caused by any motion through an intergalactic medium as may be indicated by the small deflection of the old lobes towards the west. In this example sketched here, resembling the situation of 0828+32, the precession is shown over some 40% of the precession period. The particle ages derived for the outer tips of the lobes then suggest a precession period of $\sim$ 0.2 Gyr. Another candidate source for the scenario described above is the FRII source 3C223.1 (see Black 1992).

3.3. Summary and conclusions

We have derived the distribution of the spectral index across ten low- or intermediate-luminosity (the latter are also 4C sources) radio sources selected from the B2 catalog. For the low-luminosity sources, partly published maps at λ49 cm obtained with the WSRT were compared with data at λ2.8 cm which were obtained with the Effelsberg 100-m telescope. In case of the 4C sources, we utilized published VLA measurements at λ20 cm. Because of the angular resolution of 69″, limited by the high-frequency observations with the 100-m, it is the large-scale components of these objects which are investigated in this study.

Four of the sample sources, viz. 0326+39, 0836+29, 1243+26, 1615+35, and 1827+32, exhibit a spectral index distribution which may be considered as 'normal' for this kind of radio source: the spectra are rather flat in the central regions, with values in the range of $\alpha = -0.2 \cdots -0.5$; they steepen

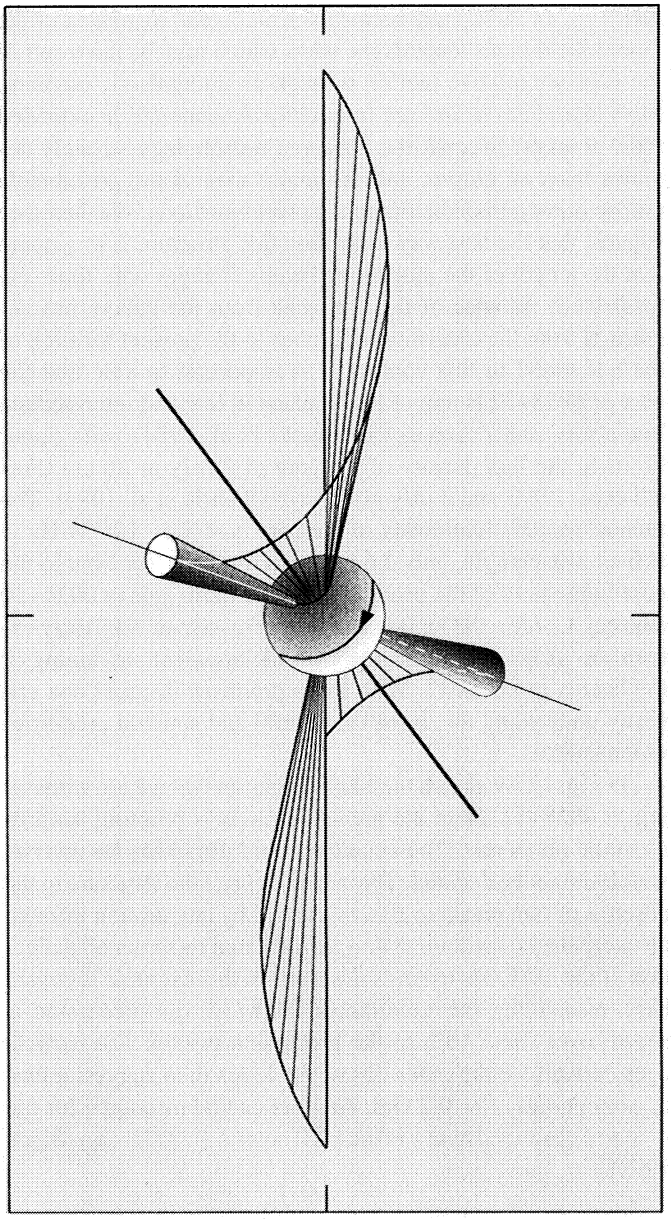

Fig. 12. Three-dimensional sketch of the precessing, shortening beam of 0828+32

towards the outer lobes where $< \alpha >= -0.8 \cdots -1.0$. The flat spectra are the result of beam smearing of the cores, which often have very flat synchrotron self-absorbed spectra, plus the inner jet regions which have flatter spectra than the outer lobes. The latter show clear signs of particle ageing, especially at high radio frequencies.

The particle ages derived here are in the range of 40 to 70 Myr. for most of the sources. Comparison with FRII sources shows that the steepening of the spectra in low-luminosity radio galaxies is not as strong as expected on the basis of studies of 3C radio galaxies (see e.g. Alexander & Leahy 1987). Classical FRII radio galaxies appear to have break frequencies between about 1 and 5 GHz, while about half of our sample shows break frequencies higher than this. This could indicate significant re-acceleration in low-luminosity radio galaxies to take place.

The spectral index behaviour in 0136+39 is, however, rather different: the spectrum steepens from the outer lobes *inwards*, thus mimicking the typical behaviour of FRII sources. However, the range of spectral indices ($< \alpha >= -0.9$ in the lobes, $< \alpha >= -1.7$ towards the core) suggests a rather aged FRII type source.

In 0204+29 the observed spectral index distribution is strongly affected by at least one unrelated background source, rendering an overall steepening of the spectrum from one end of the source to the other. It is likely that the source has little intrinsic spectral variation if the background source is accounted for. Rather little spectral variation is also seen along the major axis of 1321+31, with changes in the spectral index of at most 0.1 between $\lambda\lambda 49$ and 2.8 cm. A clear steepening is seen though perpendicular to the source axis. Together with the perfectly perpendicular magnetic field in this source this suggests a significant particle flow away from the jet.

The presumed head-tail nature of the source 2249+37 lends further support from our spectral index map, which indicates a steepening of the spectrum from the proposed core of this source towards the likely outer tails. The complex structure of 2249+37 necessitates, however, measurements at higher resolution which should become feasible in the near future with the new $\lambda 9$ mm system which is being installed in the secondary focus of the 100-m telescope.

The source 0828+32 is a rather special case. We propose a model in which its unusual radio morphology, along with the conspicuous weakness of the core, is interpreted in terms of a precessing jet, the length of which has decreased strongly over the last $\sim 2 \cdot 10^8$ yr. Our spectral index distribution corroborates this model, with a continuous spectral steepening from the young inner to the old lobes which emerge at nearly right angles from the source major axis. Thus, 0828+32 is one of the rare cases in which the history of the activity of the central engine has been 'painted' onto the sky. In view of the paucity of genuine relic radio sources, i.e. sources which obviously possess old lobes and which lack detectable cores and jets the scenario proposed here may help to tackle questions concerning radio source life times, gas supply of the central machines in radio galaxies, and time scales of radio source exhaustion.

We finally point out that the spectral indices derived here are obtained over a wide frequency range, with only two observing frequencies involved. This implies that the true high-frequency spectrum may actually be steeper than that obtained in this study. The problem is that for radio sources of $5'$ or more angular extent, maps at intermediate frequencies, e.g. 5 GHz, suffer from poor angular resolution if obtained with a single dish, and are strongly affected by the lack of zero-spacings if observed with aperture synthesis telescopes. Future measurements at $\lambda 9$ mm with the 100-m telescope are mandatory. In order to more accurately determine the particle and hence source ages it is indispensible to incorporate measurements at such short wavelengths.

Acknowledgements. UK and KHM are indebted to the Istituto di Radioastronomia del CNR in Bologna for the warm hospitality during various visits. Part of this work was supported by the Deutsche Forschungsgemeinschaft, grant KL533/4–1.

References

Alexander P. 1987, MNRAS 225, 27
Alexander P., Leahy J.P. 1987, MNRAS 225, 1
Andernach H., Feretti L., Giovannini, G. Klein U., Rosetti E., Schnaubelt J. 1992, A&AS 93, 331
Black A.R.S., 1992. In: Roland J. et al. (eds.) Extragalactic Radio Sources – From Beams to Jets. Cambridge Univ. Press, p. 302
Bondi M., Gregorini L., Padrielli L., Parma P. 1993, A&AS 101, 431
Bridle A.H., Baum S.A., Fomalont E.B., Fanti R. Parma P., Ekers R.D. 1991, A&A 245, 371
Carilli C.L., Perley R.A., Dreher J.W., Leahy J.P. 1991, ApJ. 383, 554
Colla G., Fanti C., Fanti R., Gioia I., Lari C., Lequeux J., Lucas R. Ulrich M.-H. 1975, A&AS 20, 1
Cordey R.A., 1987 MNRAS 227, 695
Ekers R.D., Fanti R., Lari C., Ulrich M.-H. 1978, A&A 69, 253
Ekers,R.D., Fanti R., Lari C., Parma P., 1981 Nat 276, 588
Ekers R.D., Fanti R., Lari C., Parma P., 1981 A&A 101, 194
de Ruiter H.R., Parma P., Fanti C., Fanti R. 1986, A&AS 65, 111
Fanti C., Fanti R., Gioia I.M., Lari C., Parma P. Ulrich M.-H., 1977, A&AS 29, 279
Fanti R. Lari C., Parma P., Ekers R.D. 1981a, A&A 94, 61
Fanti R. Lari C., Parma P., Bridle A.H., Ekers R.D., Fomalont E.B. 1981b, A&A 110, 169
Fanti C., Fanti R., de Ruiter H.R., Parma P., 1986 A&AS 65, 145
Fanti C., Fanti R., de Ruiter H.R., Parma P., 1987 A&AS 69, 57
Feretti L., Giovannini G., Gregorini L., Parma P., Zamorani G. 1984, A&A 139, 55
Gregorini L., Padrielli L., Parma P., Gilmore G., 1988 A&AS 74, 107
Gregorini L., Klein U., Parma P., Schlickeiser R., Wielebinski R. 1992, A&AS 94, 13 (Paper I)
Jägers W.J. 1986, Ph.D. thesis, Univ. of Leiden
Jaffe W.J., Perola G.C. 1973, A&A 26, 423
Kardashev N.S. 1962, Sov. Astron. AJ 6, 317
Katgert-Merkelijn J., Lari C., Padrielli L. 1980, A&AS 40, 91
Katz-Stone D.M., Rudnick L., Anderson C. 1993, ApJ 407, 549
Leahy, J.P., Muxlow, T.W.B., Stephens, P.W. 1989, MNRAS 239, 401
Leahy J.P., Parma P. 1992. In: Roland J. et al. (eds.) Extragalactic Radio Sources – From Beams to Jets. Cambridge Univ. Press, p. 307
Liu, R., Pooley, G., Riley, J.M. 1992, MNRAS 257, 545
Machalski J., Condon J.J. 1985, AJ 90, 5
Mack K.-H., Gregorini L., Parma P. Klein U., 1994, A&AS 103, 157 (Paper II)
Meurs E.J.A., Unger S.W. 1981, A&AS 45, 99
Meurs E.J.A., Unger S.W. 1991, A&A 252, 63
Miley G. 1980, ARA&A 18, 165
Myers S.T., Spangler S.R. 1985, ApJ 291, 52
Pacholczyk A.G. 1970, Radio Astrophysics. Freeman, San Francisco
Pacholczyk A.G. 1977, Radio Galaxies. Pergamon, New York
Parma P., Ekers R.D., Fanti R., 1985, A&AS 59, 511
van der Laan, H., Perola, G.C. 1969, A&A 3, 468
Wehrle A.E., Preston R.A., Meier D.L. et al., 1984, ApJ 284, 519

This article was processed by the author using Springer-Verlag TEX A&A macro package 1992.